

**DESIGNING A DETECTION METHOD OF  
CHERENKOV RADIATION USING SMARTPHONE-  
BASED CMOS CAMERA**

**MUHAMMAD ZAIM SYAMIL BIN ZAMRI**

**SCHOOL OF HEALTH SCIENCES**

**UNIVERSITI SAINS MALAYSIA**

**2020**

**DESIGNING A DETECTION METHOD OF  
CHERENKOV RADIATION USING SMARTPHONE-  
BASED CMOS CAMERA**

**By**

**MUHAMMAD ZAIM SYAMIL BIN ZAMRI**

Dissertation submitted in partial fulfillment

of the requirements for the degree of

Bachelor of Health Science (Honours) (Medical Radiation)

July 2020

## **DECLARATION**

I hereby declare that this dissertation was the result of my own investigations, except where otherwise stated and duly acknowledged. I also declare that it has not been previously or concurrently submitted as a whole for any other degrees at Universiti Sains Malaysia or other institutions. I grant Universiti Sains Malaysia the right to use the dissertation for teaching, research and promotional purposes.

.....  
Muhammad Zaim Syamil Bin Zamri

Date: 4<sup>th</sup> August 2020

## **ACKNOWLEDGEMENT**

First of all, I would like to express my upmost gratitude to Allah S.W.T for all the blessings He has given to me to complete this final year research project regarding ‘Designing a Detection Method of Cherenkov Radiation Using a Smartphone-Based CMOS Camera’. I am indeed very thankful for it.

Secondly, I would like to give my thanks to Professor Ahmad bin Zakaria, as our research coordinator, who has been giving his endless support and guidance throughout this journey. I would also like to give my special thanks to my supervisor, Dr Muhammad Nur Salihin bin Yusoff for his guidance, encouragement, endless support, supervision and handful of valuable suggestions towards completing this project. Furthermore, I am very grateful and thankful to have Mr. Ahmad Thaifur bin Khaizul, my project co-supervisor, for his endless support, valuable help, and guidance during the practical of this project specifically although that the department was quite pack on the schedule.

Lastly, I send my regards and blessing towards all of those who cooperated and support me throughout this project; my family for their endless motivation and support and especially my friend Muhammad Ariff Luqman bin Khalid for his help during the completion of my thesis. Words cannot explain how indebted I feel to them and I would love to repay their kindness in forthcoming days.

## TABLE OF CONTENT

<b>CERTIFICATE</b> .....	ii
<b>DECLARATION</b> .....	iii
<b>ACKNOWLEDGEMENT</b> .....	iv
<b>LIST OF FIGURES</b> .....	vii
<b>LIST OF TABLES</b> .....	ix
<b>LIST OF ABBREVIATIONS</b> .....	x
<b>LIST OF SYMBOLS</b> .....	xii
<b>ABSTRAK</b> .....	1
<b>ABSTRACT</b> .....	3
<b>CHAPTER 1: INTRODUCTION</b> .....	4
1.1 Background of Study .....	4
1.2 Problem statement.....	8
1.3 (a) Main Objective .....	8
1.3 (b) Specific Objectives.....	8
1.4 Scope of Research.....	9
1.5 Outline of Thesis.....	9
<b>CHAPTER 2: LITERATURE REVIEW</b> .....	10
2.1 Image Sensor.....	10

2.1.1 Charge-coupled device (CCD).....	10
2.1.2 Complimentary metal-oxide semiconductor (CMOS).....	12
2.2 A Review on Design and Instrumentation for Detecting CR .....	14
<b>CHAPTER 3: METHODOLOGY .....</b>	<b>21</b>
3.1 Materials .....	21
<b>CHAPTER 4: RESULTS .....</b>	<b>32</b>
4.1 Application of Photo-Kako software .....	32
4.2 Application of an endoscope.....	32
4.3 Application of a Realme C2.....	34
<b>CHAPTER 5: DISCUSSION .....</b>	<b>35</b>
5.1 Analysis of result .....	35
5.2 Challenges and limitations .....	36
<b>CHAPTER 6: CONCLUSION .....</b>	<b>38</b>
6.1 Conclusion .....	38
6.2 Recommendation for Future Research .....	38
<b>REFERENCES.....</b>	<b>39</b>
<b>APPENDICES.....</b>	<b>41</b>
Appendix A. Readings of Radioactivity by Dose Calibrator.....	41

## LIST OF FIGURES

Figure 1.1	Illustration of the creation of CR. (Alaeian, 2014).
Figure 1.2	Example of CR occurrence. (D.V Skryabin et al., 2017)
Figure 1.3	Example of Cherenkov Luminescence Imaging (CLI) depicted from (Robertson et al., 2009)
Figure 2.1	Illustration of CCD workflow. Depicted from parenthesis.com.
Figure 2.2	Illustration of CMOS workflow. Depicted from parenthesis.com.
Figure 2.3	Schematic figure of the lens-coupled CCD system. Depicted from (Cho et al., 2009)
Figure 2.4	A schematic diagram of the IVIS 200 Vivo Vision System (Xenogen). (Spinelli et al., 2010).
Figure 2.5	Experimental set up used by (Hammarstedt, 2019)
Figure 3.1	Realme C2 smartphone
Figure 3.2	1.5ml centrifuge tube
Figure 3.3	Tube holder
Figure 3.4	Atomlab™ 500 Dose Calibrator
Figure 3.5	Endoscope camera
Figure 3.6	Black bin
Figure 3.7	Photo-Kako software interface
Figure 3.8	USB camera application interface
Figure 3.9	Experimental set up with a Realme C2 smartphone
Figure 3.10	Experimental set up with an endoscope attached to the Realme C2

- Figure 4.1 (a) Image of a smartphone screen in a dark environment (black bin).
- Figure 4.1 (b) The image was converted to red-blue color coded heatmap using Photo-Kako software.
- Figure 4.2 Raw data image captured by OEM endoscope with using USB Camera application on Android 9.0 system.
- Figure 4.3 Converted heatmap image by using 'photo-kako' heatmap converter software.
- Figure 4.4 (a) Image of a dark system environment (black bin).
- Figure 4.4 (b) Converted image from Figure 4.3(a) to red-blue color coded heatmap using Photo-kako software.



## **LIST OF TABLES**

- Table 2.1    Advantage and disadvantage of CCD and CMOS image sensor.
- Table 2.2    Comparison of design, methods, and instrumentation from previous studies.

## **LIST OF ABBREVIATIONS**

CR	Cherenkov Radiation
PET	Positron Emission Tomography
SPECT	Single-Photon Emission Computed Tomography
CLI	Cherenkov Luminescence Imaging
CMOS	Complimentary Metal-Oxide Semiconductor
CCD	Charge-Coupled Device
MOSFET	Metal-Oxide Semiconductor Field Effect Transistor
ADC	Analog to Digital Converter
DAC	Digital to Analog Converter
ICCD	Intensified Charge-Coupled Device
EMCCD	Electron Multiplying Charge-Coupled Device
DQE	Detective Quantum Efficiency
PDMS	Polydimethylsiloxane
CE	Cherenkov Effect/ Cherenkov Emission
FWHM	Full Width at Half Maximum
PMT	Photomultiplier Tubes
PDAF	Phase Detection Auto Focus
FPS	Frames Per Seco
OI	Optical Imaging
IVIS	In Vivo Imaging System

HD	High Definition
MP	Mega Pixel
CPU	Computer Processing Unit
GB	Gigabytes
RAM	Random Access Memory

## LIST OF SYMBOLS

$^{99m}\text{Tc}$	Technetium-99m
$^{131}\text{I}$	Iodine-131
$^{18}\text{F}$	Flourine-18
$^{64}\text{Cu}$	Copper-64
$^{89}\text{Zr}$	Zirconium-89
$^{124}\text{I}$	Iodine-124
$^{225}\text{Ac}$	Actinium-225
$^{90}\text{Sr}$	Strontium-90
$^{68}\text{Ga}$	Galium-68
$^{13}\text{N}$	Nitrogen-13
$\alpha$	Alpha
$\beta^-$	Electron
$\beta^+$	Positron
$\gamma$	Gamma

## ABSTRAK

**Latar belakang:** Sinaran Cherenkov (CR) telah diguna pakai secara mendalam pada kaedah kajian masa kini. Fenomena ini mempunyai potensi untuk menjadi salah satu alternatif yang lebih menjimatkan dan praktikal pada teknologi perubatan nuklear semasa, seperti pengimejan PET dan SPECT. Walau bagaimanapun, kewujudan fenomena ini dan aplikasinya masih lagi tidak diketahui ramai. **Matlamat:** Tujuan eksperimen ini adalah untuk mereka sebuah sistem dan instrumentasi yang sesuai untuk mengesan CR dari teknetium-99m dan Iodin-131 menggunakan semikonduktor oksida logam bercas (CMOS) dari telefon pintar dan endoskop. **Bahan dan kaedah:** Lima tiub yang mengandungi teknetium-99m dengan jumlah radioaktiviti berbeza (disusun dalam bekas) dan kemudiannya diletak dalam bekas hitam yang berisi air. Imej latar belakang dan CR ditangkap dengan menggunakan telefon pintar Realme C2 dan kamera endoskopi. Kemudian ia diubah kepada peta haba berwarna menggunakan perisian “photo-kako” untuk analisis CR. **Keputusan:** Pencahayaan berjaya dikesan oleh kamera CMOS, dan imej ditukar kepada peta haba berwarna. Intensiti piksel yang tertinggi dapat dilihat pada aktiviti  $545\mu\text{Ci}$  diikuti oleh  $163\mu\text{Ci}$ ,  $113,5\mu\text{Ci}$ ,  $42\mu\text{Ci}$ , dan  $28,5\mu\text{Ci}$ . Walau bagaimanapun, kehadiran cahaya dari luar masih dapat dikesan dalam sistem kerana keadaan sistem yang tidak stabil untuk mengekalkan persekitaran yang kalis cahaya luar. **Konklusi:** Melalui perbandingan reka bentuk sistem berasaskan kajian terdahulu, kami dapat membangun sebuah sistem yang mampu mengesan cahaya menggunakan kamera CMOS berasaskan telefon pintar. Walau bagaimanapun, kehadiran cahaya pada imej berasaskan teknetium-99m bukanlah fenomena Cherenkov kerana ia tidak mempunyai ciri-ciri sebagai salah satu pemancar Cherenkov. Namun begitu, penghasil zarah

tenaga tinggi seperti Iodin-131 dapat menghasilkan CR dan oleh itu dicadangkan untuk dikaji dalam kajian masa hadapan.

## ABSTRACT

Cherenkov radiation (CR) has been exploited in various applications in modern research. It has potential to be a cost-efficient and practicable alternative to the current nuclear medicine technology such as PET and SPECT imaging. However, the existence of Cherenkov phenomenon and its application was not well known. The aim of this experiment was to design methods for detecting CR from Tc-99m and Iodine-131 using a low-cost CMOS camera from smartphone and endoscope. Tc-99m with five different radioactivity were inserted into five separate tubes (arranged in holder) and then submerged under the water in a dark environment of closed black bin. Images of both background and CR were captured using a Realme C2 smartphone and an endoscope cameras. The images were then converted to a color coded heatmap using photo-kako software for CR analysis. The luminescence detected by the CMOS camera was converted to a color coded heatmap using the photo-kako software. The highest intensity of pixel was located at isotope with an activity of 545 $\mu$ Ci followed by 163 $\mu$ Ci, 113.5 $\mu$ Ci, 42 $\mu$ Ci, and 28.5 $\mu$ Ci respectively. However, the ambient light was still presence due to instability of the system to retain a light-tight environment. Through comparison of how the set up was designed on the previous studies, we were able to construct a system to detect CR using a smartphone-based CMOS camera. However, the luminescence detected in the Tc-99m system was not a Cherenkov phenomenon as it does not have the characteristic of a Cherenkov emitter. On the other hand, high energy charged particles emitter such as Iodine-131 is recommended to be studied in future research for CR detection.

# CHAPTER 1: INTRODUCTION

## 1.1 Background of Study

The first discovery of Cherenkov Radiation (CR) was found by Pavel Cherenkov in 1934. During a radioactive preparation of an experiment, he saw a faint bluish light presence in the water bottle, with further research he concluded that it was not a fluorescent phenomenon. A theory of this effect was later developed in 1937 by his colleagues Igor Tamm and Ilya Frank (Cherenkov, 1937).

CR occurs when the velocity of a charged particle exceeds the speed of light in a dielectric medium. A charged particle moving at relativistic speed induces a temporary electric field and will disrupt the structure of medium or polarizing it. As the medium returns to its original state and the electrons fall back to its lower energy, photons were emitted with an energy proportional to the energy in the atom.

For a particle which travels at a higher velocity than the speed of light, constructive interference occurred, creating amplified waves of light distributing themselves spherically. The multiple spheres created as the particle moves through the medium add up, creating a cone of light. This light formation was to be known as Cherenkov radiation (Olausson, 2012). As in Figure 1.1, the edge of the cone travels in unity in the direction of the yellow arrow, which was dependent on the angle of distribution. The angle of distribution,  $\theta$  at which the radiation was diffracted was dependent on the velocity,  $v$  as well as the wavelength,  $\lambda$ , which



described in **equation 1**, assuming that  $P_0$  is the momentum of particle,  $c$  is the speed of light,  $m_0$  is the rest mass of the particle,  $h$  is the Planck's constant and  $v = c/n\lambda$ .

$$\cos \theta = \frac{2(P_0^2 c^2 + m_0^2 c^4)^{\frac{1}{2}} + (n^2 - 1)h\nu}{2P_0 cn} \quad (1)$$

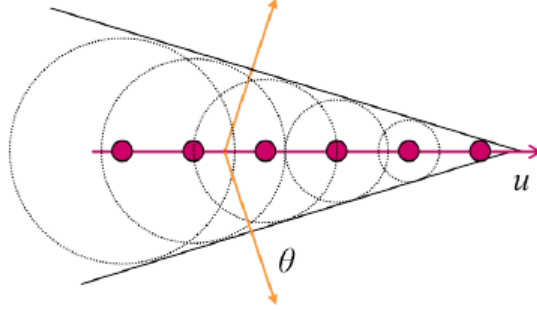


**Figure 1.1:** Illustration of the creation of CR. Depicted from (Alaeian, 2014).  $\theta$  represent the angle of distribution and  $u$  is the particle velocity.

Since the distribution of light was dependent on the wavelength,  $\lambda$ , light with shorter wavelengths will cause a higher value of  $\cos \theta$ ; thus, the distribution of shorter wavelengths was more significant than that of longer ones. Blue light with shorter wavelengths ( $<450\text{nm}$ ) than the ones towards the red light ( $>700\text{nm}$ ) will tend to be at the edges of the cone, thus hiding the red photons and the CR appears blue (Cherenkov, 1958). It was also due to the number of photons created at different wavelengths. An example of CR phenomenon is shown in Figure 1.2.

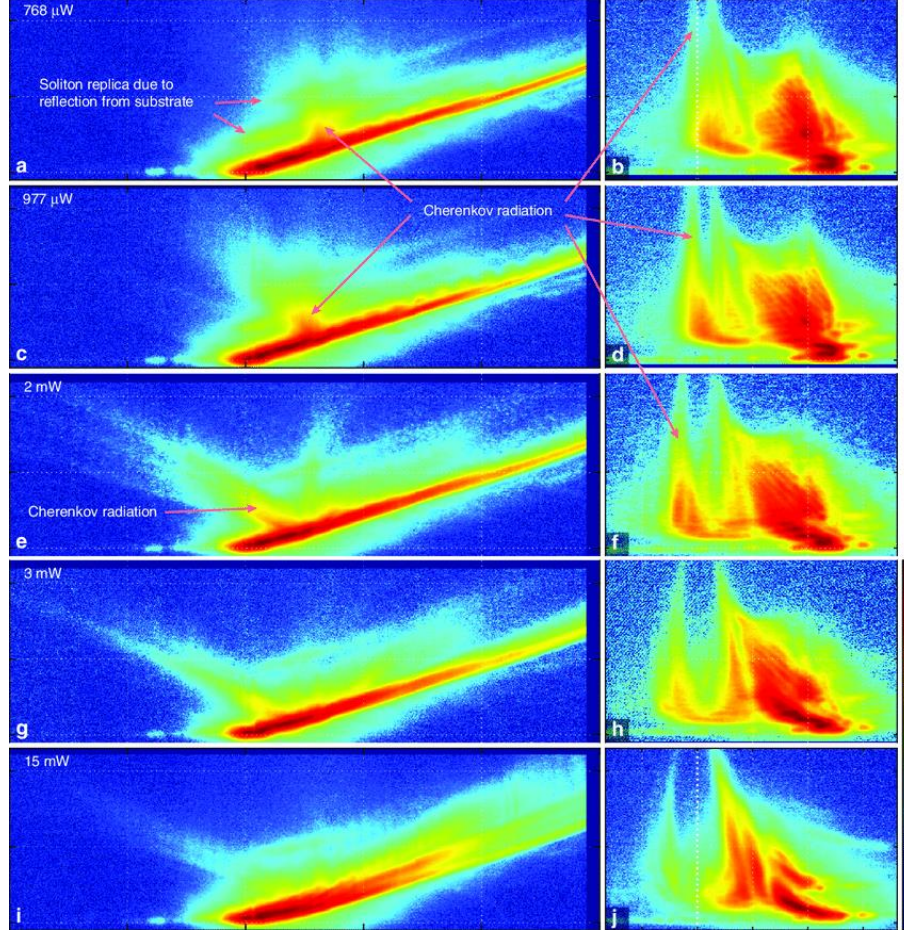


**Figure 1.2:** Example of CR occurrence. (D.V Skryabin et al., 2017)

According to **equation 2**, more photons were created in the blue light spectra than in the longer wavelength spectrum.

$$\frac{dN}{dx} = 2\pi\alpha \left( 1 - \frac{1}{\left(\frac{v}{c}\right)^2 n^2} \right) \int_{\lambda_2}^{\lambda_1} \frac{1}{\lambda^2} dy \quad (2)$$

**Equation 2** assumes that  $\alpha$  was the fine structure constant  $1/137$ ,  $n$  was the index of refraction of the material and  $\lambda$  was the wavelength in the interval  $\lambda_1$  to  $\lambda_2$  (Mitchell et al., 2011)

The CR phenomenon has numerous substantial applications in current medical research. Positron Emission Tomography (PET), or Single-Photon Emission Computed Tomography (SPECT) were used in diagnosing cancer. In both cases, radioactive materials were injected into the patient's body. The radioisotope labeled with monoclonal antibodies that bind to specific receptors will then attach and accumulates by the targeted organ to observe the tumor.

However, optical imaging (OI), which uses visible light to obtain a detailed images of organs and tissue, was both more accessible and less expensive but has been impossible due to the destruction of the light (Olausson, 2012). With the discovery of CR, Cherenkov luminescence imaging (CLI) seems to be a possible solution as an OI tool. CLI provides painless, non-invasive examinations of living organism's images that express the distribution of specific genes, cells, and proteins (Mitchell et al., 2011).

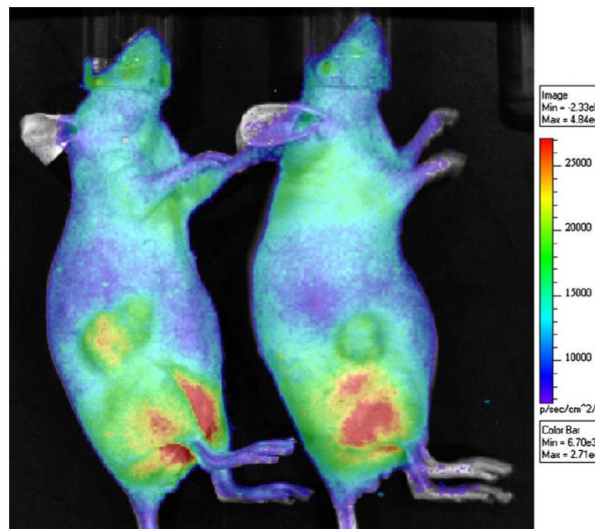


**Figure 1.3:** Example of Cherenkov Luminescence Imaging (CLI) depicted from (Robertson et al., 2009)

## **1.2 Problem statement**

The method of detecting Cherenkov radiation in current time was quite expensive, inaccessible, and complicated. It requires the application of charged coupled device (CCD) which is bulky and expensive to observe the CR phenomenon. The lack of more straightforward detection methods creates an imbalance when in comparison to the demand of the phenomenon in modern research. With the help of today's technology, the smartphone has improved quite significantly as compared to their predecessor and were known to have much faster data readout. The application of smartphone in detecting Cherenkov radiation has proved to be quite a new context in this research area. Therefore, with further adjustment and experimentation, we might be able to set up an experimental design that was stable for detecting Cherenkov radiation using a smartphone.

### **1.3 (a) Main Objective**

The aim of this study was to set up a suitable and stable experimental design to detect Cherenkov radiation by using a CMOS in a cellphone camera.

### **1.3 (b) Specific Objectives**

- I. To compare methods and instrumentations used for detecting Cherenkov radiations based on previous studies.
- II. To set up a detection system of detecting CR using Realme C2 smartphone for Tc-99m and I-131.
- III. To generate a color coded heatmap for Cherenkov radiation analysis.

## **1.4 Scope of Research**

This research will compare on other previous experimental design to set up a suitable system to detect Cherenkov radiation by mainly using a smartphone with an addition of endoscope in a laboratory. The source used were comprised of Tc-99m and Iodine-131. The aspect of the research was focusing on the application of a CMOS image sensor as a type of Cherenkov radiation detecting method.

## **1.5 Outline of Thesis**

The study was divided into several chapter starting from introduction, literature review, methodology, results, discussion, and conclusion. Appendices would include raw data from the study after the conclusion.

For the introduction, a description of the background of the study as well as the research objectives and problem statement were stated concisely. Next, in the literature review, summary and critique of what other similar research to the context of the research topic; comparison of choosing a suitable image sensor as well as different study design were summarized intensively. In methodology, materials used with all the process conducted to create a stable design would be explained as well as the description of data gathering method.

In the next chapter, the result consists of extensive description of the data imaged while in the discussion, the data were elaborately discussed and compared to other previous studies. The advantages and disadvantages of the system was presented in term of practicality with its limitations.

## **CHAPTER 2: LITERATURE REVIEW**

### **2.1 Image Sensor**

An image sensor works by detecting and conveying the information acquired to create an image. Variety of light waves are converted into signals which is referred to as a small burst of current that conveys the information. Image sensors is used in electronic imaging devices such as digital cameras, camera modules, camera phones, and medical imaging equipment. The two main types of electronic image sensors were the charge-coupled device (CCD) and the complimentary metal-oxide semiconductor (CMOS) sensor. Both CCD and CMOS sensors were based on metal-oxide semiconductor (MOS) technology with CCD based on MOS capacitors and CMOS based on MOS field-effect transistor (MOSFET) amplifiers. The advantage and disadvantage of CCD and CMOS are shown in Table 2.1.

#### **2.1.1 Charge-coupled device (CCD)**

In a CCD, there was a photoactive region and a transmission region made of a shift register. An image captured was projected through a lens onto the capacitor array (photoactive region), causing each capacitor to accumulate electric charge proportional to the light intensity at that location. Then, the control circuit would cause the content in each capacitor to be transferred to the shift register. The charge collected will then be amplified and be converted into a voltage via the Analog to Digital Converter (ADC) as shown in Figure 2.1.

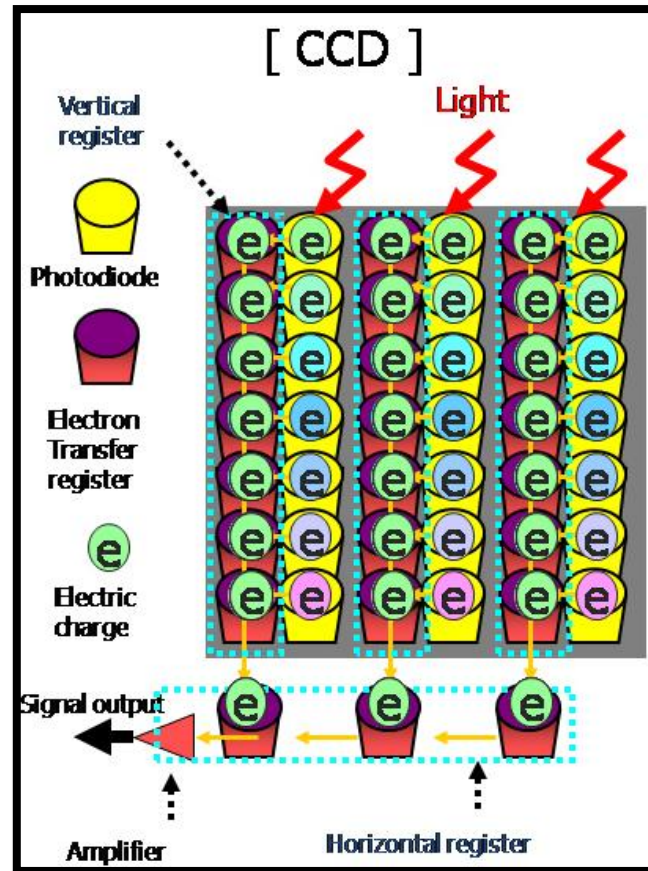
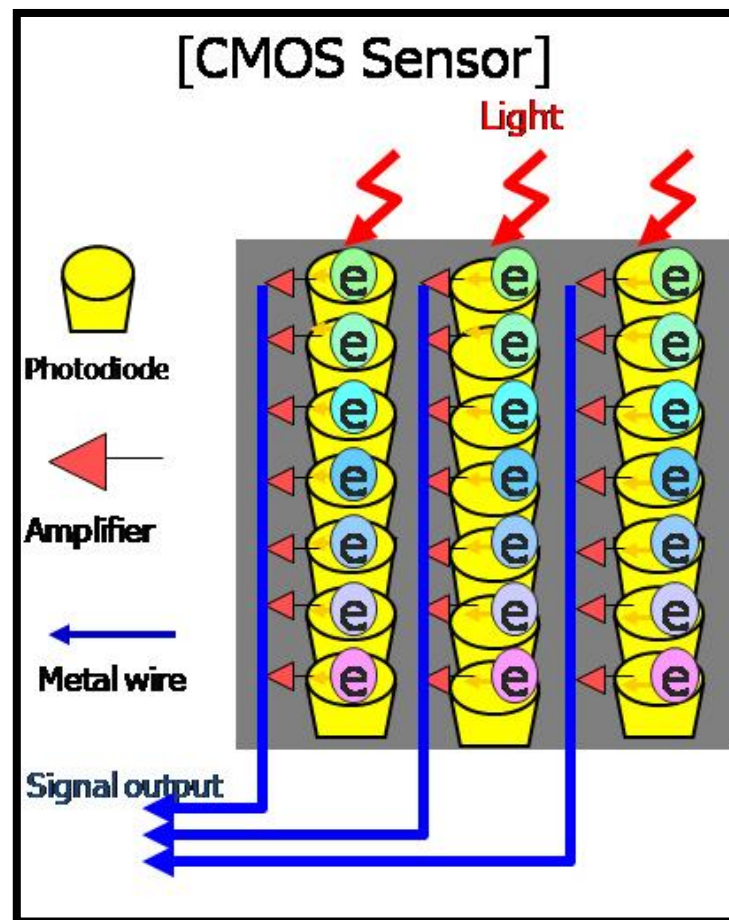


Figure 2.1: Illustration of CCD workflow. Depicted from parenthesis.com.



### 2.1.2 Complimentary metal-oxide semiconductor (CMOS)

In a CMOS sensor, the signal was multiplexed by row and column to multiple on-chip digital to analog converters (DACs) once the charge from the photosensitive pixel was converted to a voltage at the pixel site. Each site was essentially a photodiode and three transistors, performing the functions of resetting or activating the pixel, amplification and charge conversion, and selection or multiplexing as can be seen in Figure 2.2.



**Figure 2.2:** Illustration of CMOS workflow. Depicted from parenthesis.com.



**Table 2.1:** Advantage and disadvantage of CCD and CMOS image sensor.

CCD	CMOS
Higher image quality because it has an individual amplifier that amplified the transmitted data uniformly.	Lower image quality as it contains many amplifiers resulting in non-uniform data transmission.
Low image noise due to uniform data transmission.	High image noise due to non-uniform data receives.
High dynamic range	Low dynamic range
Presence of blooming effect. Occurs due to spillage of charge from one photosensitive site to the neighbouring sites which is caused by finite well depth.	Rolling shutter effect tends to occur when capturing a fast moving object, creating a disoriented representation of the image.
Bulky because the ADC was unable to be integrated into a CCD sensor.	Small form factor as the ADC was able to be integrated into one small chip.
Higher power consumption. Due to the requirement of different power supply for different timing clocks in a CCD sensor.	Low power consumption. It only require a single power supply to operate.

In a study done by Andreozzi et al., several sensors were compared and tested out to select the suitable in vivo detector of Cherenkov radiation (CR). The sensor includes CMOS, CCD, intensified CCD (ICCD), and electron-multiplying ICCD (EM-ICCD). The key factors that were used for the comparison: (i) low light sensitivity or detective quantum efficiency (DQE), (ii) ambient light rejection, and (iii) frame rate capability. The group of five sensors were split into two groups: standalone (CMOS, CCD) and intensified (ICCD, EM-ICCD). The standalone images were processed with temporal median filtering, background

subtraction, as well as spatial median filtering. The result shows that the standalone detectors (CMOS and CCD) were not adequate for real-time tissue imaging. However, the effect of CR may be captured by the CMOS or CCD using an optically transparent and less absorptive medium such as water or doped fluorescent molecule (Glaser et al., 2014). The study showed that CMOS and CCD sensor types were feasible to be used in detecting CR, thus paving the way for low-cost Cherenkov optical imager in the future. The application of the Cherenkov phenomenon might replace the current system such as PET or SPECT, which was known for its high cost of maintenance. Furthermore, with such low-cost technology, it will expand the availability to every laboratory or facility hence increasing the patient throughput.

## **2.2 A Review on Design and Instrumentation for Detecting CR**

(Cho et al., 2009) was the first to describe the use of CR light for direct optical imaging using a CCD from the observations of beta particles in a microfluidic chip. The experiment uses  $^{18}\text{F}$ , which decays through the emission of high-energy positrons and the energy threshold to generate CR was calculated for water and polydimethylsiloxane (PDMS). A broad distribution from 300nm to 700nm was observed from the emitted light of the  $^{18}\text{F}$  with higher intensity at shorter wavelengths. A bluish-white light was observed from the solution, which suggesting the occurrence of the Cherenkov effect (CE) (Cho et al., 2009). The design of CCD set up for this experiment was depicted in Figure 2.3. The work done in this experiment proves that beta particles emitted from  $^{18}\text{F}$  generate visible light, which was consistent with the characteristics of CR, and the signal can be detected by using a lens-coupled CCD system.

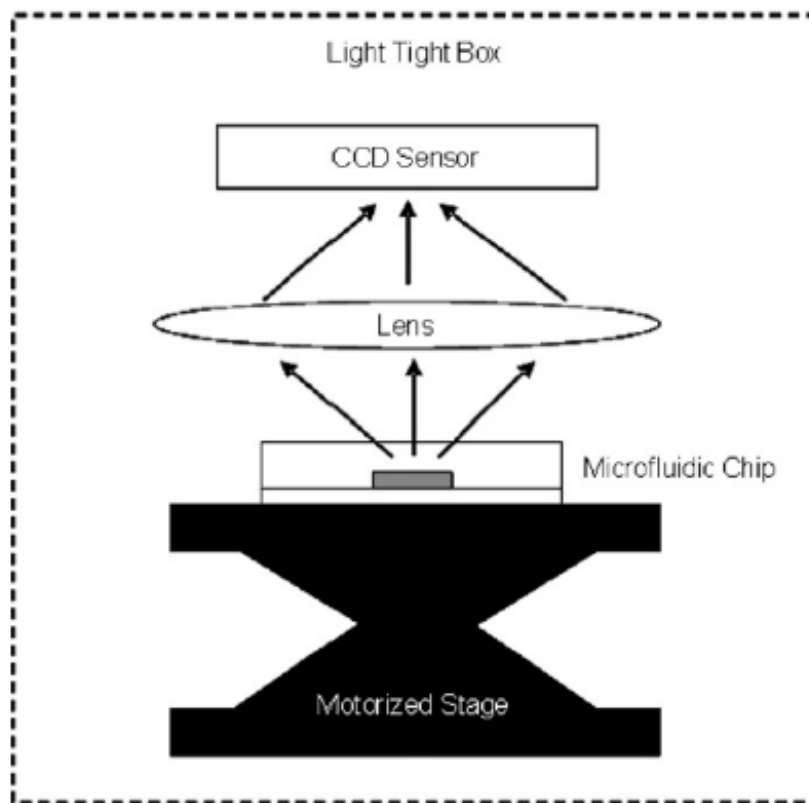


**Figure 2.3:** Schematic figure of the lens-coupled CCD system. Depicted from (Cho et al., 2009).

In the same year, Robertson et al. published a research proving the principle of *in vivo* studies. The preliminary demonstration showed that they successfully detected luminescence signals from high-energy positron emitters that were  $^{18}\text{F}$  and  $^{13}\text{N}$  (both nuclides have maximum  $\beta^+$  energy that exceed the Cherenkov threshold). The images were captured using a CCD image sensor, Xenogen IVIS, without any fluorescence filters or an external excitation source. Furthermore, a positive correlation was shown between the measured CCD signal and the refractive index of the medium. Light output also corresponded to the inverse squared of the wavelength, which prove that it was consistent with CR. Through this finding, they coined the term Cherenkov luminescence imaging (CLI) for this novel molecular imaging

method in which visible light emission from CR was detected during the decay of positron-emitting radionuclides (Robertson et al., 2009).

Spinelli et al., had conducted a research about the application of CR for *in vivo* optical imaging of positron-emitting radiotracers. In their work, they used a CCD as an optical imager, specifically an IVIS 200 system. The system was composed of a back-thinned, back-illuminated CCD camera with a lens and several filters: wide band filters with full-width at half maximum (FWHM) greater than 50nm, narrowband filters with FWHM approximately equal to 20nm. The full set up of their system was shown in Figure 2.4. Before any images were acquired, they measured a dark image and used it to subtract the values from the acquired image. The result was significant for future research as it proved the possibility of detecting CR from positron-emitting radionuclides such as  $^{18}\text{F}$  and  $^{68}\text{Ga}$  using standard optical imaging techniques and the possibility to obtain *in vivo* Cherenkov images in small animals using a conventional optical imaging system (Spinelli et al., 2010).

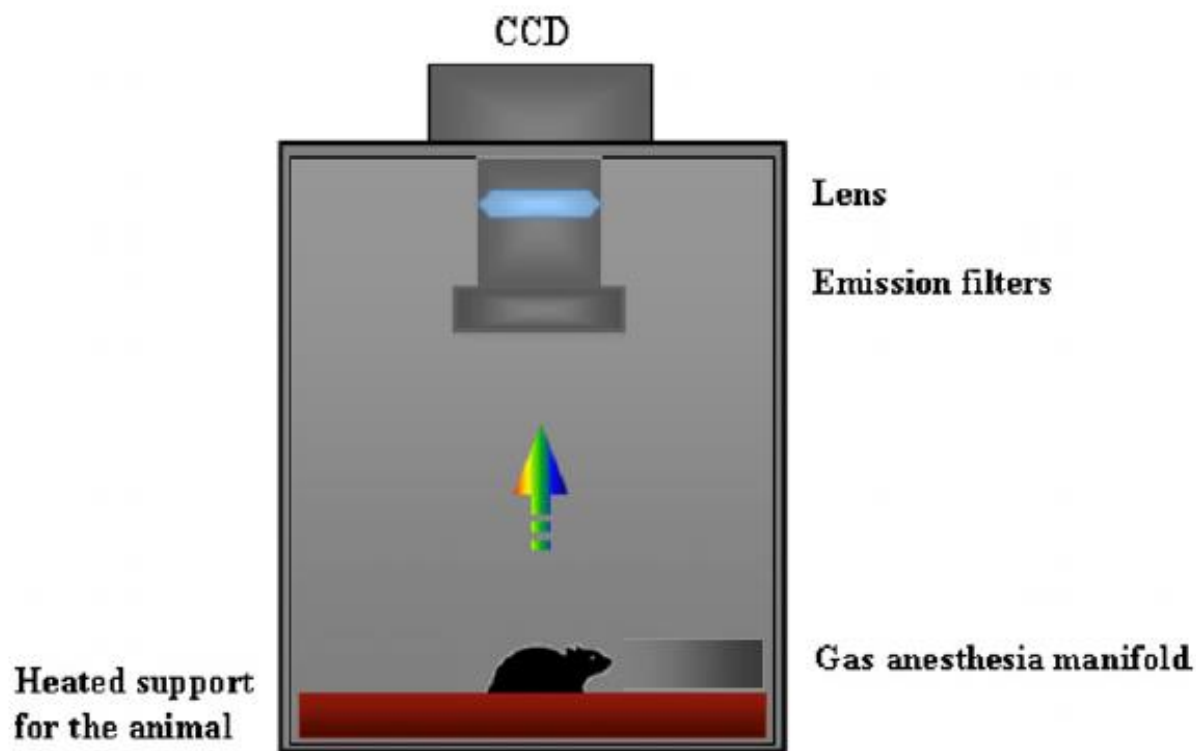


**Figure 2.4:** A schematic diagram of the IVIS 200 Vivo Vision System (Xenogen). Depicted from (Spinelli et al., 2010).

In addition, Ruggerio et al. has demonstrated the feasibility of detecting CR in not only positron emitters ( $^{18}\text{F}$ ,  $^{64}\text{Cu}$ ,  $^{89}\text{Zr}$ ,  $^{124}\text{I}$ ) but also  $\beta$ -emitter ( $^{131}\text{I}$ ) and the potential of  $\alpha$ -emitter which was  $^{225}\text{Ac}$  use in CLI. The radionuclides were studied by phantoms with varying activity concentration. The phantoms were imaged using the IVIS 200, which was using a CCD image sensor. They found that clinically used radionuclides were able to be visualized, and the data obtained correlate with the observed biodistribution of radiotracers. This proves that not only positron can be applied in CLI but also  $\beta$  and  $\alpha$  emitter can be applied as well.

The study of Cherenkov detection by a CMOS was done a decade later, and it was demonstrated by Ellen Hammerstedt with the use of cellphone as an alternative method in detecting CR. The project was tested out with a  $^{90}\text{Sr}$  radionuclide, which undergoes  $\beta^-$  decay. Prior to detecting the CR with a cellphone, he creates a system to investigate whether there was any possibility of detecting any signals under the circumstantial conditions. Once the requirement for a functional system were identified, the PMT was replaced by a cellphone.

He tested out three cellphones in particular: Iphone8+, Huawei Honor 7, and a Samsung Galaxy S3 mini, which in his suggestion that the latter was best suited for the experiment followed by Honor 7. The experimental set up when using the cellphone was shown in Figure 2.5. For the experiment, three videos were collected (6-minutes long); two with CR-source present and a background light.

The result show that the CR was able to be detected by a cellphone; Honor 7 calibrate some of its background light, causing it to detect less blue light. He emphasizes that the system needs to be properly darkened to avoid any background light contamination to produce a good result. The finding of this project fills the gaps, where the CR can be detected by a CMOS sensor, which was cheaper and compact than a CCD sensor.

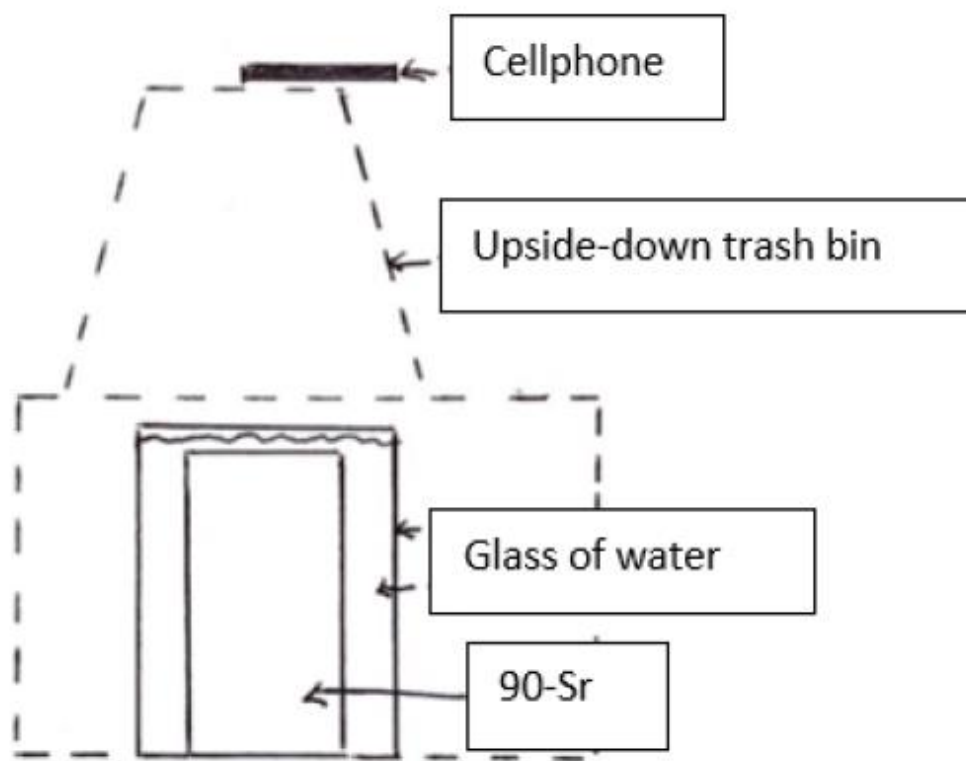


**Figure 2.5:** Experimental set up used by (Hammarstedt, 2019)

**Table 2.2:** Comparison of design, methods, and instrumentation from previous studies.

Research title	Type of Image sensor	Design/Method	Source used	Finding
Cerenkov radiation imaging as a method for quantitative measurements of beta particles in a microfluidic chip. (Cho et al., 2009)	CCD	Lens with a focal length of 25mm was mounted below the CCD sensor. Set up was placed in a light-tight box. Lens-object distance at 5.7cm. Image-to-object magnification was 0.3.	- $^{18}\text{F}$	Positron generate CR and can be detected by a CCD image sensor
Optical imaging of Cerenkov light generation from positron-emitting radiotracers. (Robertson et al., 2009).	CCD	Wells of $^{18}\text{F}$ and $^{13}\text{N}$ with activity of 1, 10, 100 $\mu\text{Ci}$ scanned with integration time of 10s using bioluminescence channel. Performed scan with opaque paper to confirm the detected signal was visible light. Tested out with $^{99\text{m}}\text{Tc}$ and no light detected.	- $^{18}\text{F}$ , $^{13}\text{N}$	Termed Cherenkov Luminescence Imaging Higher refractive index of the medium, higher CR signal obtained
Cerenkov radiation allows in vivo optical imaging of positron emitting radiotracers. (Spinelli et al., 2010)	CCD	IVIS 200 set at bioluminescence mode was used without any excitation lamp. System comprises of back-thinned, back-illuminated CCD camera, several filters and lens. Dark measures were obtained prior to image acquisition.	- $^{18}\text{F}$ , $^{68}\text{Ga}$	Feasible of detecting CR from $^{18}\text{F}$ and $^{68}\text{Ga}$ using standard optical imaging Possibility to obtain <i>in vivo</i> CR in small animal
Cerenkov luminescence imaging of medical isotopes. (Ruggerio et al., 2010)	CCD	Images were acquired using Xenogen IVIS 200 with integration time of 10, 20, 30, 40, 50 and 60s in bioluminescence setting. No light interference from the excitation lamp.	- $^{18}\text{F}$ , $^{64}\text{Cu}$ , - $^{89}\text{Zr}$ , $^{124}\text{I}$ ( $\beta^+$ ) - $^{131}\text{I}$ ( $\beta^-$ ) - $^{225}\text{Ac}$ ( $\alpha$ )	Feasible of detecting CR from clinically used radionuclides and the data measured correlate with observed biodistribution of radiotracers.
Detecting Cherenkov radiation with a cellphone. (Hammerstedt, 2019)	CMOS	$^{90}\text{Sr}$ was placed in the glass of water. Placed under a box with a circular hole above the glass. An upside-down trash bin was positioned to cover the hole. The system was darkened with a large black tarpaulin-like blanket.	- $^{90}\text{Sr}$	Feasible for detecting CR by using a cellphone's camera.



## **CHAPTER 3: METHODOLOGY**

### **3.1 Materials**

#### **3.1.1 Technetium-99m**

The properties of Tc-99m include the emission of gamma rays with an energy of 140 keV; with a half-life of 6 hours; and decay through an isomeric transition. In this study, we will observe and analyze whether will a Cherenkov luminescence arises from given energy.

#### **3.1.2 Iodine-131**

The properties of I-131 includes the emission of 10% gamma ray with an energy of 364 keV and 90% of the gamma ray with energy of 606 keV; with half-life of approximately 8 days; and decay through the mode of  $\beta$ -decay.

#### **3.1.3 Plain water**

The plain water was used to submerge the radionuclides, acting as a dielectric medium for this study.

### 3.1.4 Realme C2 smartphone

Realme C2 smartphone (Realme, China) as in Figure 3.1, was manufactured with a width of 73.8mm, height of 154.4mm, depth of 8.4mm, and weight of 166g. For the display, they include 15.5cm wide display with a screen and aspect ratio of 89.35% and 19.5:9 respectively; and an HD+ resolution of 1560 by 720 pixels. Ellen Hammerstedt found that the best possible result can be obtained by 5MP of camera whereas for this Realme C2, it provided dual rear camera with 13MP+2MP, which was more than suitable to be used as the primary detector. Furthermore, it also features phase detection auto focus (PDAF) fast focusing, f/2.2 aperture, and 5P lens; while for the front camera, 5MP and 1.12 $\mu$ m pixels was provided; the video can be recorded at constant 30 frames per second (fps) for a resolution of 720p or 1080p with an addition of slo-mo video software. The battery capacity of this model was about 4000mAh. It features MediaTek Helio P22, 12nm CPU technology, 2.0GHz frequency, 2GB/3GB RAM, 16/32GB ROM, and storage of up to 256GB. It currently using ColorOS 6.0 based on Android 9.0, which was compatible to be used for pairing with the endoscope.



**Figure 3.1:** Realme C2 smartphone

### 3.1.5 Centrifuge tube

1.5ml centrifuge tube, as in Figure 3.2, will be used to hold the radionuclides.



**Figure 3.2:** 1.5ml centrifuge tube

### 3.1.6 Tube rack/holder

Tube holder with the capacity to hold 72 tubes of 0.2ml-1.5ml was used to hold the tubes underwater. A weight such as lead or rock was used to keep the holder submerged during experimentation.



**Figure 3.3:** Tube holder

### 3.1.7 Dose calibrator

Atomlab™ 500 Dose calibrator (Atomlab, USA) as in Figure 3.4 was used to determine the background radiation of the hot lab and to measure the activity of radionuclides. This model can detect an activity ranging from 0.01 $\mu$ Ci to 100 $\mu$ Ci (0.0004MBq to 3700GBq) of Tc-99m or 25Ci of Flourine-18. It has energy range of 25keV to 3MeV photons. The response time was about one to two seconds for doses greater than 200 $\mu$ Ci; 3 seconds for doses greater than 20  $\mu$ Ci; 50-100 seconds below 20 $\mu$ Ci of Tc-99m with default threshold; threshold was adjustable to reduce counting time. The electrometer linearity was about  $\pm 1\%$  or 0.2  $\mu$ Ci, whichever was greater, up to 40 curies of Tc-99m,  $\pm 1.5\%$  up to 100 curies of Tc-99m while the electrometer accuracy was  $\pm 1\%$  or 0.2 $\mu$ Ci, whichever was greater. Overall accuracy was  $\pm 3\%$  or 0.3 $\mu$ Ci, whichever was greater and repeatability:  $\pm 0.3\%$  above 1mCi short term (24hr); 1% long term. The detector was a well-type pressurized ionisation chamber, filled with Argon gas. The dimension was 6-inch diameter x 15.5 inch; 25-inch lead shielding provided on all sides except the top well opening with supplementary shielding. Linearity was about  $\pm 1\%$  or 0.2  $\mu$ Ci, whichever was greater while the weight of the detector was 16 kg.



**Figure 3.4:** Atomlab™ 500 Dose Calibrator